J Toxicol Pathol 2024; 37: 39–43

Case Report

Spontaneous mandibular follicular ameloblastoma in a female Sprague-Dawley rat

Juan Li[1], Guojian Jiang[1], Jie Zhang[1], Zhuolin Ou[1], Xin Wu[1], and Yueshu Liu[1]*

[1] Department of Laboratory, Guangdong Medical Laboratory Animal Center, 119 Poyang Road, Nanhai District, Foshan 528000, Guangdong, China

Abstract: Ameloblastoma is a locally aggressive tumor derived from the odontogenic epithelium of the developing tooth germ. It is rarely reported in experimental Sprague-Dawley (SD) rats. In this 90-day percutaneous repeated-dose toxicity study, mandibular nodules were observed from day 56 to 90. Upon necropsy, a well-demarcated nodule, approximately 1.2×1.0×1.0 cm, was found attached to the mandibular bone, alongside the unerupted left incisor. Histopathologically, the epithelial cells formed islands, nests, or anastomosing strands. The epithelial islands were surrounded by a peripheral layer of tall columnar cells with antibasilar nuclei arranged in a palisading pattern. Several mitotic cells were observed. Some epithelial islands displayed cystic degenerative changes and squamous metaplasia. Necrotic tissue with inflammatory cell infiltration was observed at the tumor margins. Immunohistochemically, the neoplastic epithelial islands and mesenchymal components exhibited positivity for pan-cytokeratin and vimentin, respectively. Based on these features, the case was diagnosed as follicular ameloblastoma in an SD rat. (DOI: 10.1293/tox.2023-0072; J Toxicol Pathol 2024; 37: 39–43)

Key words: odontogenic tumor, mandible, Sprague-Dawley rat

Spontaneous ameloblastomas are rare in rats. They are chemically induced by the application of various *N-nitrosourea* derivatives[1]. Ameloblastomas are tumors originating from the epithelium of dentigerous cysts, remnants of the dental lamina and enamel organ, and the basal cell layer of the oral mucosa[2]. It has been reported in dogs[3], rabbits[4], and Wistar and Sprague-Dawley (SD) rats[5, 6]. Specifically with regard to rats, a detailed morphological description of the acanthomatous ameloblastoma was provided in a 120-week-old female Wistar rat[5]. Two additional spontaneous unclassified ameloblastomas were observed in a 30-week-old and 80-week-old SD rats from different toxicity studies[6]. Background lesions including ameloblastic carcinoma, cystic ameloblastoma, and peripheral ameloblastic odontoma have also been reported in rats[7, 8]. According to the classification of the International Harmonization of Nomenclature and Diagnostic Criteria for Lesions in Rats and Mice (INHAND), five types of ameloblastoma have been described, including follicular, plexiform, solid, cystic, and acanthomatous types[2]. However, to the best of our knowledge, the follicular ameloblastomas presented in this study have not been reported in experimental SD rats.

The purpose of this study was to present and describe a case of follicular ameloblastoma observed as an incidental finding in a 22-week-old female SD rat during a 90-day percutaneous repeated-dose toxicity study.

The 8-week-old, female specific pathogen free (SPF) SD rat was purchased from Department of Production in Guangdong Medical Laboratory Animal Center (GDMLAC, Foshan, China). The study was approved by the Institutional Animal Care and Use Committee of GDMLAC, following the national experimental animal welfare ethics review guide. After a 1-week quarantine period, the rat was served as a vehicle control in this 90-day percutaneous repeated-dose toxicity study. The study was carried out after 1 week of animal quarantine. On the day before administration, the fur on the rat's back of the rat, which accounted for approximately 10% of the body surface area, was shaved. As a part of the vehicle control group, deionized water was smeared on the rat's back skin every day. According to the national regulations on laboratory animal management, the rat was kept in an SPF facility (GDMLAC) licensed by the Guangdong Laboratory Animals Monitoring Institute. It was housed alone in a solid-bottom polycarbonate cage, under standard conditions (temperature 23 ± 3°C, humidity 55 ± 15%, and a 12-h light-dark cycle), with free access to irradiated feed and filtered tap water. The rat underwent daily clinical observation, and the tumor was measured by veterinarian once a day. At the conclusion of the 90-day study, the rat was 22-week-old. Euthanasia was performed via exsanguination of abdominal aorta under urethane (Sinopharm

Received: 2 June 2023, Accepted: 3 October 2023
Published online in J-STAGE: 13 November 2023
*Corresponding author: Y Liu (e-mail: juliegzglp@163.com)

Chemical Reagent Co., Ltd., Shanghai, China) anesthesia at a dose of 1.2 g/kg. A complete necropsy was performed under the supervision of a pathologist. The mandibular mass was fixed in 10% neutral formalin, decalcified in 10% formic acid, and dehydrated with 70% anhydrous ethanol and xylene. Subsequently, the specimen was embedded in paraffin, sectioned at approximately 4 μm thickness, and stained using hematoxylin and eosin and Masson's trichrome stain. Immunohistochemistry (IHC) was performed using antibodies against pan-cytokeratin (clone 4D11G2+7G4C9, mouse monoclonal, Servicebio, Wuhan, China) and vimentin (rabbit polyclonal, Servicebio). Negative control was not treated with primary antibody. The IHC was performed according to the protocols provided by the manufacturer. The tissue sections were examined and diagnosed under a light microscope.

The rat showed a mild decrease in food consumption and slow weight gain from days 49 to 56. The mandibular nodule was first observed on day 56 and persisted until day 90 (22-week-old). Throughout the experiment, the tumor size did not exceed 40 mm, which is within the humane endpoint limit.

Grossly, a well-demarcated nodule, approximately 1.2×1.0×1.0 cm, was found in the jaw. The nodule was grayish white, with an uneven surface and was attached to the mandibular bone, along with an unerupted left incisor (Fig. 1). The right incisor erupted in a crooked manner and was located on the right side of the mass.

Microscopically, the epithelial cells formed islands, nests, or anastomosing strands and were embedded in the interstitial tissue (Fig. 2A). The alveolar bone was visible at the bottom of the tumor (Fig. 2A, 2B). Some bone trabeculae were scattered within or around the epithelial cell nests. Both the interstitial tissue and bone trabeculae stained green with Masson's trichrome (Fig. 2B, 2C). The

Fig. 1. Gross appearance of ameloblastoma in the mandibular mass of an SD rat. An arrow points to the right incisor. The delineating line indicates the cutting direction along with the sagittal plane of the mass. Scale bar=5 mm.

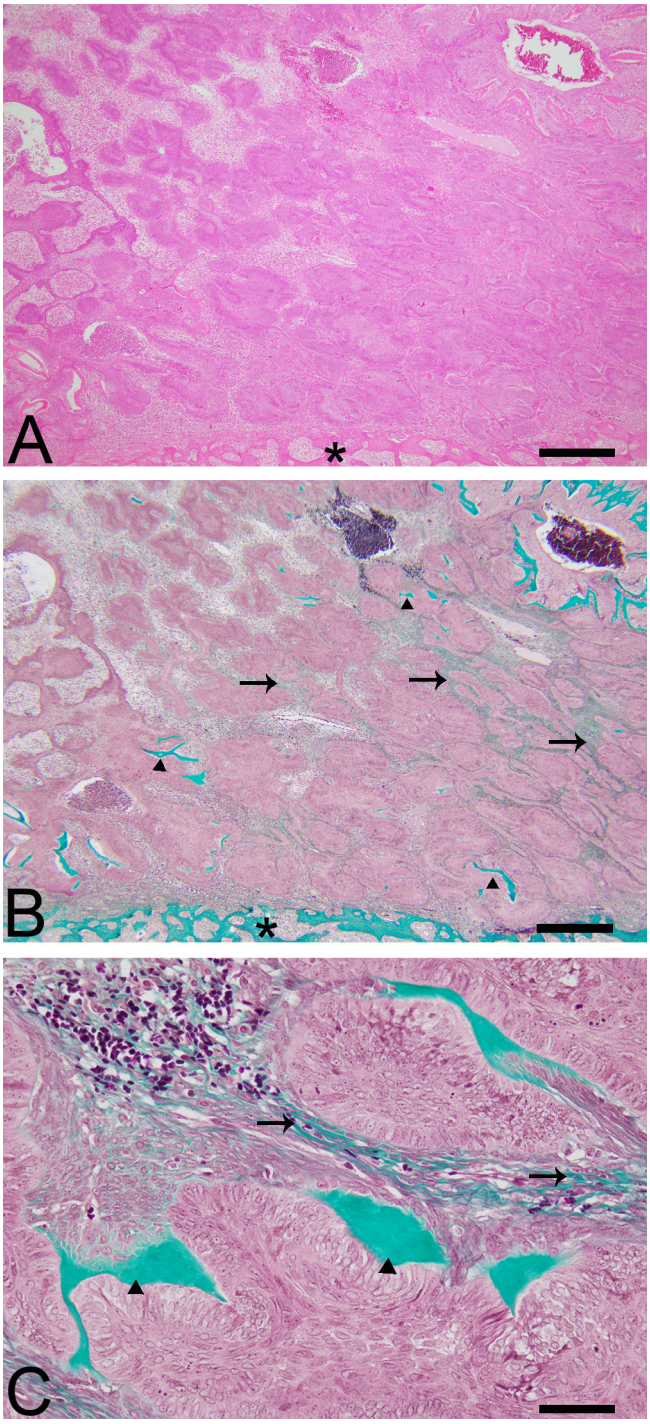

Fig. 2. Histological features of ameloblastoma in the mandibular mass of an SD rat. **(A)**Epithelial cells formed islands, nests or anastomosing strands, embedded in interstitial tissue. The alveolar bone (asterisk) is visible at the bottom of the tumor. Hematoxylin and eosin (HE) stain. Scale bar=500 μm. **(B)** Epithelial cells are surrounded by fibrous connective tissue (arrows). Some bone trabeculae (▲) are scattered within the mass. The alveolar bone (asterisk) is observed at the bottom of the tumor. Masson's trichrome stain. Scale bar=500 μm. **(C)** Fibrous connective tissue (arrows) and bone trabeculae (▲) from Fig. 2B are observed at higher magnification. Masson's trichrome stain. Scale bar = 50 μm.

formation of odontogenic hard tissues, such as enamel and dentin, was not apparent in the tumor. The tumor cells aggressively invaded the surrounding jawbones. Necrotic tissue with inflammatory cell infiltration was observed at the tumor margins. The surrounding nests of tumor cells contained moderate numbers of neutrophils and macrophages. The epithelial islands were surrounded by a peripheral layer of tall columnar cells with antibasilar nuclei arranged in a palisading pattern (Fig. 3A, 3F). Several forms of central cells were observed within epithelial islands. Centrally, the epithelial cells were arranged loosely with long intercellular bridges, resembling the stellate reticulum, or clustered densely, resembling the basal cells (Fig. 3A, 3 B). These were the dominant types of tumor cells. Additionally, some

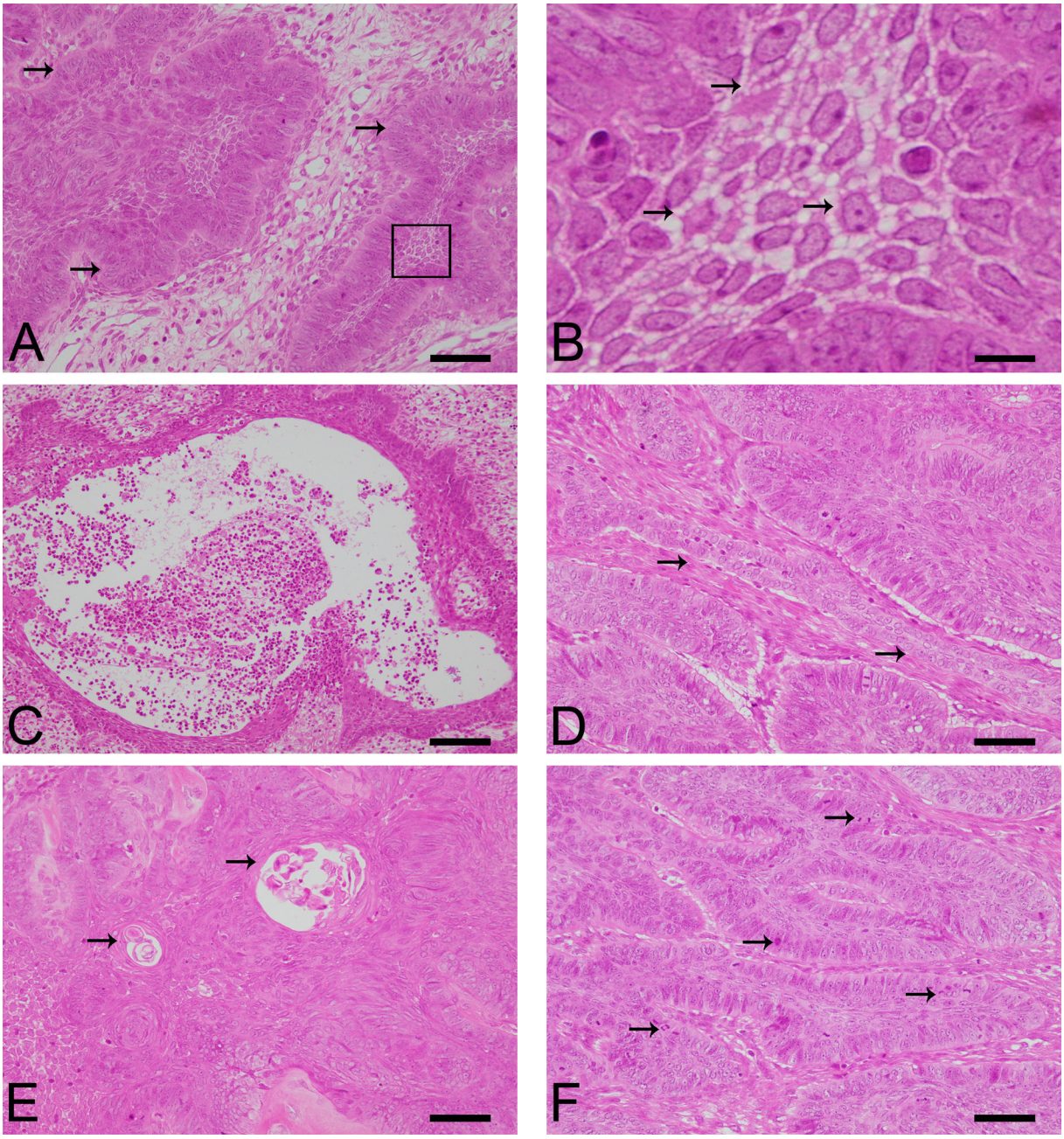

Fig. 3. Histological features of ameloblastoma in the mandibular mass of an SD rat with hemotoxylin and eosin stain. **(A)** Cuboidal to tall columnar epithelial cells forms a peripheral palisade (arrows). Central epithelial cells are arranged loosely, resembling stellate reticulum, and/or clustered densely, resembling basal cells. The square indicates the specific region being magnified in Fig. 3B. Scale bar=50 µm. **(B)** Stellate reticulum cells with long intercellular bridges (arrows) from Fig. 3A are observed at higher magnification. Scale bar=10 µm. **(C)** Areas of cystic degeneration, necrotic tissue, bleeding, and inflammatory cell infiltration. Scale bar=100 µm. **(D)** Epithelial cells show plexiform pattern (arrows). Scale bar=50 µm. **(E)** Epithelial islands show squamous metaplasia with keratin pearl formation (arrows). Scale bar=50 µm. (**F**) Tall columnar epithelial cells form peripheral palisade with numerous mitotic figures (arrows). Scale bar=50 µm.

epithelial islands showed cystic degeneration, hemorrhage, and necrosis (Fig. 3C). Some epithelial cells were arranged in a cord-like manner between epithelial islands (Fig. 3D). In addition, squamous metaplasia was observed in some epithelial cell islands (Fig. 3E). The squamous cells grew concentrically with keratin pearl formation on the tumor islands (Fig. 3E). The atypical cell nuclei were round to oval with clear membranes and nucleoli. Numerous mitotic figures were observed (Fig. 3F). No distant metastasis was detected during the systemic histopathological examination.

The IHC results showed that the epithelial islands were weak-to-moderately positive for pan-cytokeratin in the cytoplasm and negative for vimentin (Fig. 4A), whereas the interstitial tissues, such as fibroblasts and endothelial cells, were strongly positive for vimentin in the cytoplasm and negative for pan-cytokeratin (Fig. 4B).

Ameloblastomas are classified into five types by INHAND[2]. The neoplastic epithelium consists of tall peripheral columnar cells and loosely arranged central cells embedded in the collagenous stroma. The peripheral and central cells are the inner enamel epithelium and stellate reticulum epithelium, respectively. According to the morphological characteristics of the tumor cells, ameloblastomas were described as follicular, plexiform, solid, cystic, and acanthomatous types. The follicular type consists of numerous epithelial islands in the peripheral layer of tall columnar cells, with antibasilar nuclei arranged in a palisading pattern. The plexiform type exhibits anastomosing strands of epithelial cells. In the solid-type, the epithelial islands appear solid. In the cystic type, epithelial islands may show degenerative changes in the stellate cells, resulting in cyst formation. In the acanthomatous type, the epithelium of the stellate reticulum may undergo squamous metaplasia. Ameloblastomas are usually large, concentrically growing, locally aggressive, and destructive, but they do not metastasize. The stroma may be focally hyalinized. Additionally, dental hard tissues, such as enamel, dentin, or cementum, are usually not produced. In ameloblastomas, mixtures of different histological types are frequently observed, and lesions are commonly classified based on the predominant pattern present[9].

In this case, the neoplastic epithelium formed round-to-irregular follicles, separated by interlinking bands of fibrous stroma. The follicles contained central epithelial cells that were arranged loosely with long intercellular bridges, resembling the stellate reticulum, or were clustered densely, resembling the basal cells. These were the dominant types of tumor cells. Notably, various patterns including follicular, plexiform, acanthomatous, and basal cell patterns were observed within the tumor. In addition, some central cystic degeneration was present. The IHC results showed that the epithelial components were positive for pan-cytokeratin and negative for vimentin, whereas the mesenchymal components were positive for vimentin and negative for pan-cytokeratin. These IHC findings and diagnostic features include palisading tall columnar cells with antibasilar nuclei and centralized stellate reticulum-like cells are similar to the primary odontogenic features. In addition, some bone trabeculae were scattered within or around epithelial cell nests. The architecture of the jawbone was destroyed by the proliferative epithelium, leading to the appearance of bone trabeculae in the nodule. The tumor showed aggressive behavior, but no metastases were observed in the local lymph nodes or distant organs.

In this 90-day percutaneous repeated-dose toxicity study, tumors were not detected in the other rats except this one. Based on these diagnostic features, the lesion was diagnosed as a spontaneous follicular ameloblastoma in an SD rat.

Ameloblastomas are benign epithelial odontogenic tumors of the jaw in human[10]. They exhibit aggressive local behavior with slow growth and accounts for approximately 10% of all odontogenic tumors in the jaw[11].

In this study, care was taken to distinguish ameloblastoma from odontoma, ameloblastic odontoma, odontogenic fibroma, and malignant ameloblastoma. The features of

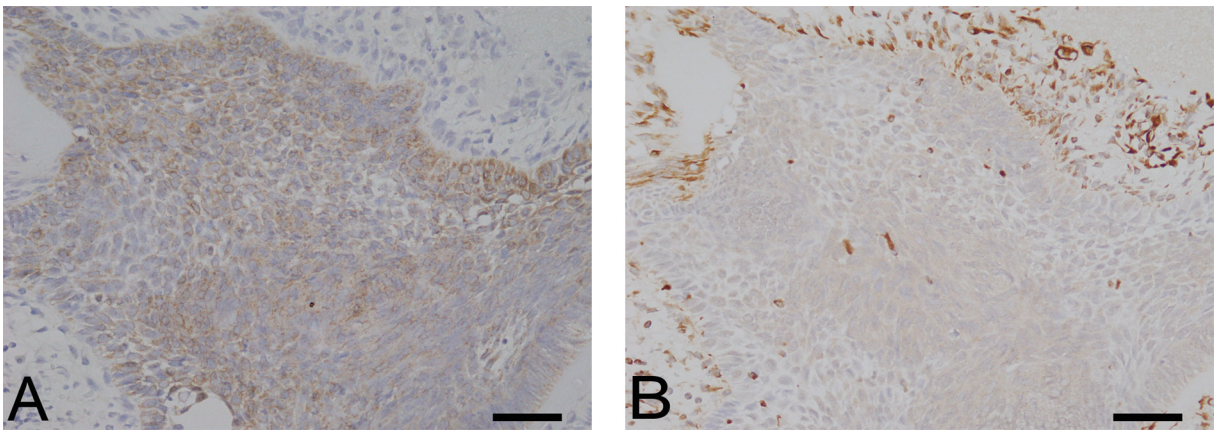

Fig. 4. Immunohistochemical staining of ameloblastoma in the mandibular mass of an SD rat. **(A)** Epithelium islands show weak-to-moderate cytoplasmic positivity for pan-cytokeratin. Scale bar=50 μm. **(B)** Interstitial tissues show strong cytoplasmic positivity for vimentin. Scale bar=50 μm.

ameloblastomas have been described in the earlier section. The difference between odontoma, ameloblastic odontoma, odontogenic fibroma, and malignant ameloblastoma can be summarized as follow[2]. Odontomas are developmental hamartomas composed of differentiated mineralized dental hard tissues that lack significant amounts of ameloblastic or ameloblastoma-like epithelia. Ameloblastic odontomas often exhibit aggressive behavior, with proliferating ameloblastic (ameloblastoma-like) epithelium located at the tumor periphery and minimal or no dental hard tissue surrounding the tumor. The formation of hard dental tissue occurs within the central area of the tumor. Odontogenic fibromas are benign, locally expansive neoplasms composed of dental follicle-like mesenchyme, and do not show enamel or dentin formation. Malignant ameloblastomas are histologically typical ameloblastomas that often metastasize to local lymph nodes or distant organs.

In the rat, the tumor was attached to the mandibular bone, alongside the unerupted left incisor. Therefore, the tumor was completely dissected along with the jawbone and teeth. Histopathologically, the peripheral epithelium consisted of tall columnar cells, similar to the inner enamel epithelium. The central cells of epithelial islands arranged loosely resembling the stellate reticulum. These features are consistent with those of the odontogenic tissue. Some central cells of the epithelial islands were clustered densely, resembling basal cells. In addition, ulceration was observed at the tumor margins, and the squamous epithelial mucosa surrounding the tumor was normal. In the absence of significant destruction of existing alveolar bone continuity, neoplastic epithelium could be observed under the alveolar bone. Moreover, no obvious continuity was observed between the tumor cells and neighboring normal oral mucosa. Only a few cysts were observed in the tumor. Based on these features, we speculated that the tumor's origin was unlikely to be from the epithelium of dentigerous cysts or basal cell layer of the oral mucosa. According to the existing literature, the epithelial dental lamina gives rise to the preameloblasts, stratum intermedium, and stellate reticulum[12]. Therefore, we speculated that the tumor in this case most likely spontaneously arose from remnants of the dental lamina or enamel organ, which resulted in the left incisor becoming slanted to the right, being embedded next to the tumor.

In addition, no ameloblastomas have been listed in the National Toxicology Program (NTP) historical database of Harlan-SD rats[13]. In the future, documenting the incidence of ameloblastoma as a spontaneous lesion will be beneficial. This case provided a reference for understanding the incidence of ameloblastoma. In addition, the typical morphology of ameloblastomas in SD rats warrants further study. We hope that this report will be helpful for understanding and identifying dental tumors in rats.

Disclosure of Potential Conflicts of Interest: The authors declare that they have no conflicts of interest.

Acknowledgments: We thank Jiarong Yan and Caixia Lou for their support. This study was supported by the Guangdong Medical Laboratory Animal Center.

References

1. Kimura A, Yoshizawa K, Sasaki T, Uehara N, Kinoshita Y, Miki H, Yuri T, Uchida T, and Tsubura A. *N-methyl-N-nitrosourea*-induced changes in epithelial rests of Malassez and the development of odontomas in rats. Exp Ther Med. **4**: 15–20. 2012. [Medline] [CrossRef]
2. Fossey S, Vahle J, Long P, Schelling S, Ernst H, Boyce RW, Jolette J, Bolon B, Bendele A, Rinke M, Healy L, High W, Roth DR, Boyle M, and Leininger J. Nonproliferative and proliferative lesions of the rat and mouse skeletal tissues (bones, joints, and teeth). J Toxicol Pathol. **29**(Suppl): 49S–103S. 2016. [Medline] [CrossRef]
3. Malmberg JL, Howerth EW, Powers BE, and Schaffer PA. Acanthomatous ameloblastoma with atypical foci in five dogs. J Vet Diagn Invest. **29**: 154–159. 2017. [Medline] [CrossRef]
4. Völker I, Kammeyer P, Hinzmann B, Lüerssen D, Baumgärtner W, and Wohlsein P. [Peripheral keratinizing ameloblastoma in a dwarf rabbit (Oryctolagus cuniculus f. dom.)]. Tierarztl Prax Ausg K Klientiere Heimtiere. **42**: 331–335. 2014 (in German). [Medline] [CrossRef]
5. Ernst H, and Mirea D. Ameloblastoma in a female Wistar rat. Exp Toxicol Pathol. **47**: 335–340. 1995. [Medline] [CrossRef]
6. Lewis DJ, Cherry CP, and Gibson WA. Ameloblastoma (adamantinoma) of the mandible in the rat. J Comp Pathol. **90**: 379–384. 1980. [Medline] [CrossRef]
7. Murphy B, Michel A, LaDouceur EB, Bell C, Lin M, and Imai DM. Ameloblastoma of the jaw in three species of rodent: a domestic brown rat (*Rattus norvegicus*), Syrian hamster (*Mesocricetus auratus*) and amargosa vole (*Microtus californicus scirpensis*). J Comp Pathol. **157**: 145–149. 2017. [Medline] [CrossRef]
8. Li Y, Bae HI, Kim HS, Kang MS, Gong BH, Jung WH, Lee S, Bae JS, Kim KH, Song SW, Lee JH, and Kang BH. Spontaneous peripheral ameloblastic odontoma in a male Sprague-Dawley rat. Toxicol Res. **33**: 141–147. 2017. [Medline] [CrossRef]
9. Masthan KMK, Anitha N, Krupaa J, and Manikkam S. Ameloblastoma. J Pharm Bioallied Sci. **7**(Suppl 1): S167–S170. 2015. [Medline] [CrossRef]
10. Nakamura N, Mitsuyasu T, Higuchi Y, Sandra F, and Ohishi M. Growth characteristics of ameloblastoma involving the inferior alveolar nerve: a clinical and histopathologic study. Oral Surg Oral Med Oral Pathol Oral Radiol Endod. **91**: 557–562. 2001. [Medline] [CrossRef]
11. Mendenhall WM, Werning JW, Fernandes R, Malyapa RS, and Mendenhall NP. Ameloblastoma. Am J Clin Oncol. **30**: 645–648. 2007. [Medline] [CrossRef]
12. Joel RL, and Melissa S. Oral cavity, teeth and gingiva. In: Boorman's Pathology of the Rat, 2nd ed. AW Suttie (ed), Academic Press, London. 15–21. 2017.
13. National Toxicology Program. NTP historical controls report all routes and vehicles Harlan Sprague-Dawley Rats. 2023. From U.S. Department of Health and Human Services website: https://ntp.niehs.nih.gov/data/controls